JOURNAL OF ENZYME INHIBITION AND MEDICINAL CHEMISTRY
2024, VOL. 39, NO. 1, 2367128
https://doi.org/10.1080/14756366.2024.2367128

Taylor & Francis
Taylor & Francis Group

RESEARCH ARTICLE

Fluorinated indeno-quinoxaline bearing thiazole moieties as hypoglycaemic agents targeting *α*-amylase, and *α*-glucosidase: synthesis, molecular docking, and ADMET studies

Nirvana A. Gohar[a], Eman A. Fayed[b], Yousry A. Ammar[c], Ola A. Abu Ali[d], Ahmed Ragab[c,e], Amal M. Mahfoz[f] and Moustafa S. Abusaif[c]

[a]Department of Pharmaceutical Organic Chemistry, Modern University for Technology and Information, Cairo, Egypt; [b]Department of Pharmaceutical Organic Chemistry, Al-Azhar University, Nasr City, Cairo, Egypt; [c]Department of Chemistry, , Al-Azhar University, Nasr City, Cairo, Egypt; [d]Department of Chemistry, College of Science, Taif University, Taif, Saudi Arabia; [e]Department for Biomaterials Research, Polymer Institute of the Slovak Academy of Sciences, Bratislava, Slovakia; [f]Department of Pharmacology and Toxicology, , Modern University for Technology and Information, Cairo, Egypt

ABSTRACT

Inhibition of α-glucosidase and *α*-amylase are key tactics for managing blood glucose levels. Currently, stronger, and more accessible inhibitors are needed to treat diabetes. Indeno[1,2-*b*] quinoxalines-carrying thiazole hybrids **1–17** were created and described using NMR. All analogues were tested for hypoglycaemic effect against STZ-induced diabetes in mice. Compounds **4**, **6**, **8**, and **16** were the most potent among the synthesised analogues. These hybrids were examined for their effects on plasma insulin, urea, creatinine, GSH, MDA, ALT, AST, and total cholesterol. Moreover, these compounds were tested against *α*-glucosidase and *α*-amylase enzymes *in vitro*. The four hybrids **4**, **6**, **8**, and **16** represented moderate to potent activity with IC_{50} values 0.982 ± 0.04, to 10.19 ± 0.21 for *α*-glucosidase inhibition and 17.58 ± 0.74 to 121.6 ± 5.14 μM for *α*-amylase inhibition when compared to the standard medication acarbose with IC_{50}=0.316 ± 0.02 μM for *α*-glucosidase inhibition and 31.56 ± 1.33 μM for *α*-amylase inhibition. Docking studies as well as *in silico* ADMT were done.

GRAPHICAL ABSTRACT

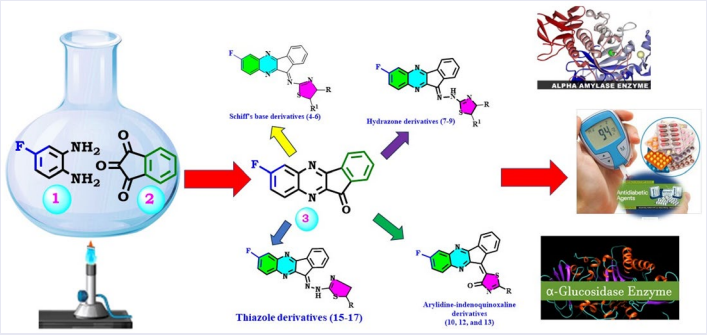

ARTICLE HISTORY
Received 13 November 2023
Revised 11 May 2024
Accepted 6 June 2024

KEYWORDS
α-Amylase; *α*-Glucosidase; Fluorinated indeno-quinoxaline

Introduction

Diabetes mellitus (DM) is becoming more and more prevalent all over the world. DM is a long-term metabolic disorder that happens when the pancreas does not make enough insulin, or the body doesn't use it adequately[1]. Almost 463 million people are affected by it globally, and by 2030, that number is predicted to reach 578 million[2]. Diabetes mellitus is a collection of metabolic illnesses defined by hyperglycaemia resulting from abnormalities in insulin secretion, insulin action, or both. Diabetes's chronic hyperglycaemia is linked to long-term harm, malfunction, and organ failure, particularly to the kidneys, eyes, heart, nerves, and blood vessels. Type II diabetes, or non-insulin-dependent diabetes mellitus (NIDDM), is characterised by impaired glucose homeostasis that leads to hyperglycaemia and is linked to neuropathy, macrovascular, and microvascular problems. NIDDM is a multifactorial, intricate disease[3].

Long-term diabetes can result in numerous problems, including alterations to the blood vessels and cellular malfunction. Proteinuria, a steady loss in renal and hepatic functioning, and a higher risk of cardiovascular illnesses are all clinical symptoms of

CONTACT Eman A. Fayed alfayed_e@azhar.edu.eg alfayed_e@yahoo.com Department of Pharmaceutical Organic Chemistry, Al-Azhar University, Nasr City , Cairo, Egypt

Supplemental data for this article can be accessed online at https://doi.org/10.1080/14756366.2024.2367128.

diabetes mellitus. Persistent hyperglycaemia boosts the formation of free radicals and weakens intracellular antioxidant defences, which causes oxidative stress and the activation of apoptotic pathways. This, in turn, controls the generation of several pro-inflammatory mediators that worsen damage to different organs and impair the course of diabetes mellitus[4–7]. Thus, creating new, safe, and biologically active anti-diabetic drugs is crucial.

Preventing problems from diabetes brought on by non-enzymatic glycation and the inhibition of blood glucose-regulating enzymes is the main objective of treatment for diabetes. The generation of insulin by pancreatic islets regulates this scenario. Furthermore, enzymes like *α* -glucosidase and *α* -amylase are employed to halt the decomposition of sugar[8]. Therefore, the inhibition of *α* -glucosidase is a major scientific focus for hyperglycaemic control in diabetic patients. Intestinal *α* -glucosidases break down dietary carbs into simple sugars so that they can be absorbed[9]. Inhibiting intestinal *α*-glucosidase is one approach of inhibiting carbohydrate breakdown and limiting carbohydrate absorption in diabetes to reduce hyperglycaemia. According to this strategy, acarbose, miglitol, and voglibose were produced as anti-diabetic medications a few years ago. However, since then, no significant development has been made in developing new *α*-glucosidase inhibitors as diabetic medications with enhanced effectiveness and fewer adverse effects[10]. To improve this area of anti-diabetic treatment, there is still a critical necessity to find novel *α* -glucosidase inhibitors to improve the activity and decrease the adverse side effects.

Moreover, the metallo-enzyme *α*-amylase is a member of the endo-amylase family and is responsible for catalysing the first step of starch hydrolysis into shorter oligosaccharides by cleaving *α*-D-(1–4) glycosidic linkages as it contains Ca2+ ions in its active site. Due to its ability to hydrolyse the 1,4-glycosidic linkage of starch and the actions that can be carried out because of hydrolysis, this enzyme attracted great interest. The use of a lot of carbohydrates is linked to certain major issues such as obesity, diabetes, and dental diseases[11–14].

Additionally, a wide variety of biological properties, for example anti-inflammatory, antibacterial, anti-cancer, and antioxidant ones, are displayed by thiazole derivatives[15]. In addition, they have been revealed to have effective α-glucosidase inhibitory action. Some examples of this activity include the thiazole derivatives isatin-thiazole[16], coumarin-thiazole[17], thiazole-pyrrole[18], and triazine-thiazole[19,20]. There is an insufficient amount of research available regarding the impact of isomerism on the inhibition of *α*-glucosidase, but those that do include research on kotalanol, iminosugars, hyacinthacins, bicyclitols, bicyclitol-deoxynojirimycin conjugates, perylene bisimide-deoxynojirimycin conjugates, perylene bisimide-deoxynojirimycin conjugates[21].

The current research is a part of our ongoing search for the discovery of novel hybrids to treat different diseases[22–27]. Herein we synthesised *α*-glucosidase and *α*-amylase inhibitors that might be used in the development of anti-diabetic medications (Figure 1).

Materials and methods

S1 in the supplementary materials[28–49].

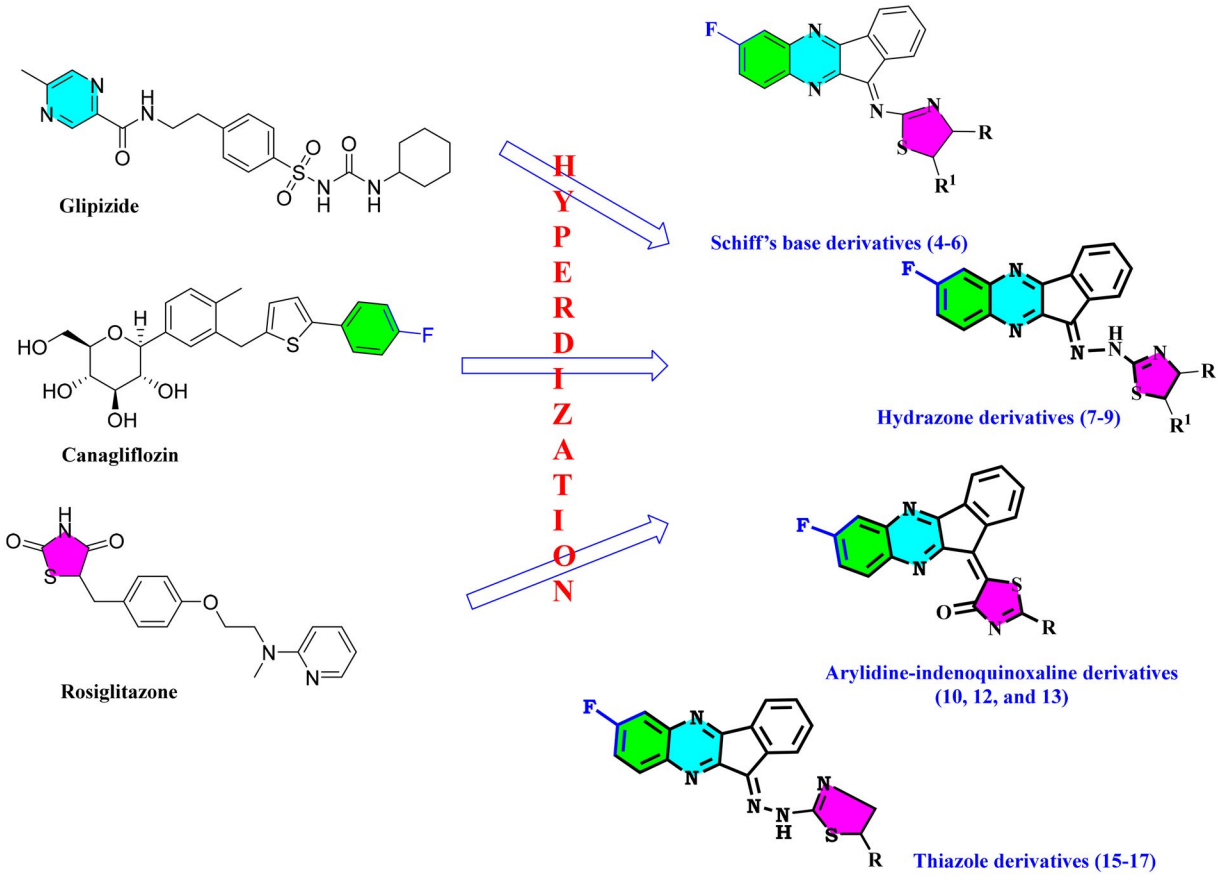

Figure 1. Synthetic approach for designing indenoquinoxaline hits **3–17**.

Result and discussion

Chemistry

All the target substances were successfully synthesised according to Scheme 1–3, and their predicted structures were validated using analytical and spectroscopic data (IR,^{1}H NMR,^{13}C NMR). According to the literature protocol[50], 7-fluoro-11*H*-indeno[1,2-*b*]quinoxalin-11-one (**3**) is prepared as a starting compound by cyclo-condensation of 4-fluoro-1,2-phenylenediamine (**1**) with ninhydrin **2** in hot methanol and catalytic quantities of acetic acid. Due to the importance of the biological activity of thiazole moiety, the author planned to design and construct a thiazole ring linked with the starting material **3** *via* keto function (C=O).

As viewed in Scheme 1, the starting material fluoro-indenoquinoxaline (**1**) was subjected to react with 2-aminothiazol derivatives specified, 2-aminothiazol-4(5*H*)-one, 1–(2-amino-4-methylthiazol-5-yl)ethan-1-one or ethyl 2-amino-4-methylthiazole-5-carboxylate via a condensation reaction to afford the corresponding imine thiazole derivatives **4–6**. The spectral data confirmed the expected structure of the products. The IR spectrum of compound **4** indicates the presence of one carbonyl group at 1736 cm^{-1} and the imino function C=N at 1604 cm^{-1}. Additionally, its ^{1}H NMR spectra designates two aliphatic protons of CH_2 at δ 4.08 ppm beside the aromatic protons ranging from δ 7.69–8.24 ppm. The^{13}C NMR spectrum revealed the aliphatic CH_2 of the thiazolone ring at δ 37.46 ppm, the aromatic carbons ranged from δ 113.94–145.60 ppm, C=N at δ 163.57 ppm, carbonyl at δ 178.41, and signals at δ 179.02 ppm due to S-C=N function. Also, the IR spectrum of compound **5** revealed an absorption band at 1735 cm^{-1} corresponding to the carbonyl group due to acetyl thiazole, while compound **6** presented absorption bands for CH aromatic, CH aliphatic, C=O, and C=N groups at 3076, 2925, 1735, 1605 cm^{-1} respectively. The ^{1}H NMR compound **5** demonstrated two singlet signals at δ 2.33, and 2.41 ppm relevant to the two methyl protons, as well as signals for the aromatic protons between δ 7.72 ppm to δ 8.25 ppm, while compound **6** displayed signals at δ 1.21, 2.38, and 4.13 ppm for two CH_3 and CH_2 of the ethyl group beside the signals of the aromatic protons. The^{13}C NMR of compound **5** characterised the structure by the presence of two signals for aliphatic carbons, signals for aromatic carbons, and signals for (C-F), and (C=O) groups.

By the same manner, 7-fluoro-11*H*-indeno[1,2-*b*]quinoxalin-11-one (**3**) was allowed to react with some thiazolyl hydrazines

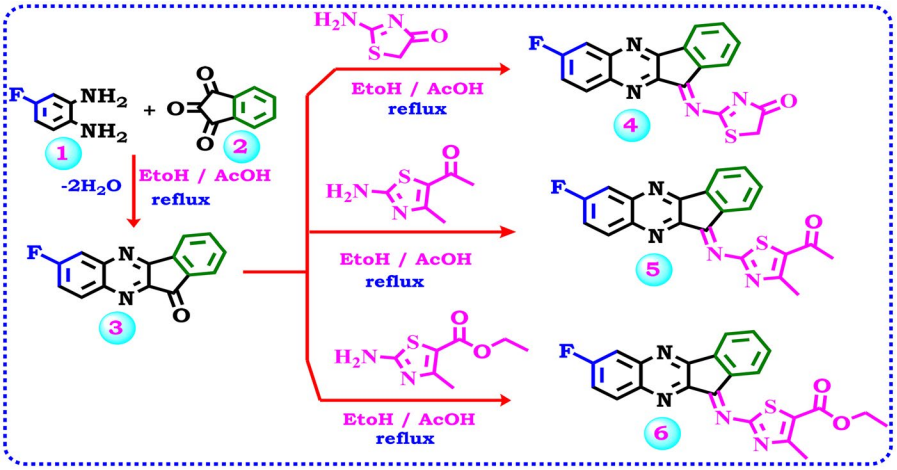

Scheme 1. Illustrate the synthesis of indeno-quinoxaline derivative **3** and synthesis of new Schiff's base derivatives **4–6**.

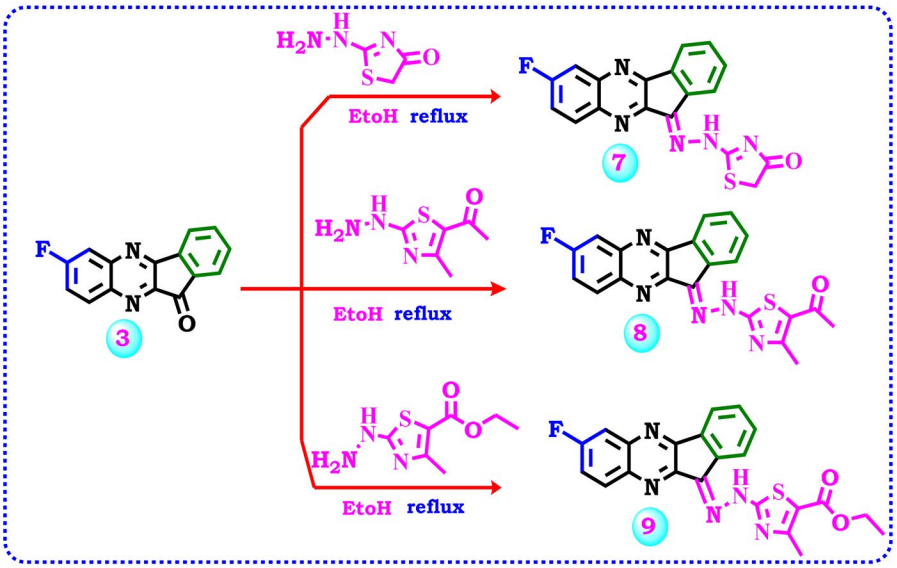

Scheme 2. Strategy for the synthesis of hydrazone derivatives **7–9**.

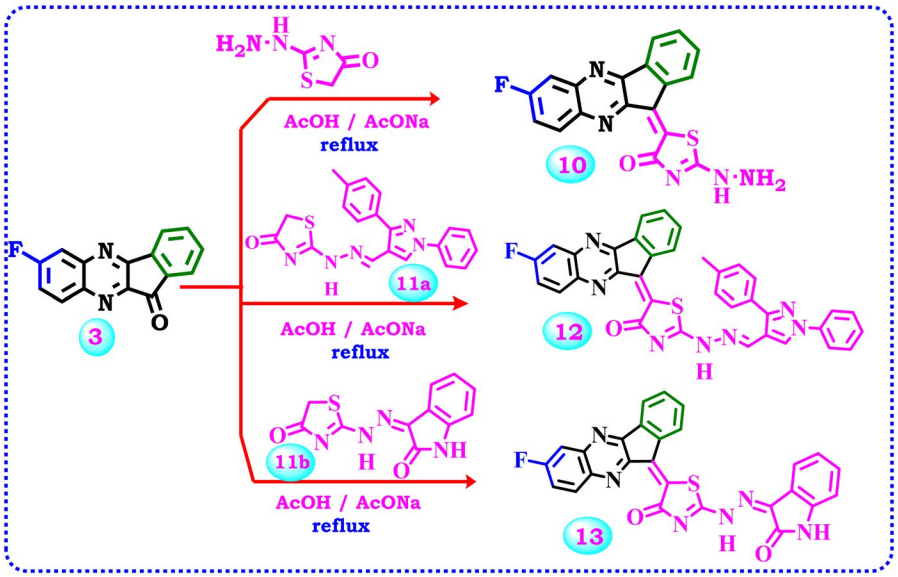

Scheme 3. Proposed reactions for the synthesis of arylidine-indenoquinoxaline derivatives **10**, **12**, and **13**.

such as 2-hydrazineylthiazol-4(5*H*)-one, 1–(2-hydrazineyl-4-methylthiazol-5-yl)ethan-1-one, or ethyl 2-hydrazineyl-4-methylthiazole-5-carboxylate, respectively, to produce the corresponding hydrazone derivatives **7–9**, Scheme 2. The IR spectrum of compound **7** revealed bands at 3130, 3049, 2967, 1709, and 1612 cm^{-1} corresponding to NH, CH-aromatic, CH-aliphatic, carbonyl, and imino (C=N) groups, respectively. Moreover, its ^{1}H NMR displayed a singlet signal at δ 4.06 ppm due to CH_2 aliphatic protons of thiazolone and one singlet signal at δ 11.77 ppm for NH beside the aromatic protons. Also, ^{13}C NMR confirmed the reaction product by the presence of a signal at δ 33.03 ppm related to CH_2 of aliphatic carbon, and twelve signals for the aromatic carbons beside the signals specific to C=N, C-F, and carbonyl carbons at δ 160.05, 162.35, and 168.75 ppm, respectively. The IR spectrum of compound **8** displayed an absorption band at 3427 attributed to (NH), and a band at 1735 cm^{-1} due to (C=O). Moreover, its ^{1}H NMR spectrum displayed two singlet signals at δ 1.94 and 2.29 ppm because of the presence of two methyl groups, a singlet signal at δ 7.96 ppm related to the NH group along with seven aromatic protons between δ 7.72 to 8.23 ppm, while ^{1}H NMR spectrum of compound **9** revealed three signals as triplet, singlet, and quartette splitting signals at δ 1.27, 2.57, 4.23 ppm which represent the aliphatic protons of methyl and ethyl groups in addition to aromatic protons and the proton of the NH group which appeared at δ 7.90 ppm. Also, the ^{13}C NMR spectrum of compound **9** displayed the existence of three carbons at δ 19.23, 21.02, and 61.94 ppm assignable for methyl and ethyl carbons in addition to the signals of the aromatic carbons and the signals representing (C=N), carbon attached to fluoride (C-F), (S-C=N), and carbonyl (C=O).

2-Hydrazineylthiazol-4(5*H*)-one has two nucleophilic active centres, hydrazine function and methylene CH_2 function. The condensation of the keto group with hydrazine function in acidic medium afforded the corresponding hydrazone, while its condensation with methylene CH_2 function in a basic medium, afforded the corresponding arylidine derivatives (C=C). Therefore, the starting material **3** was condensed with 2-hydrazineylthiazol-4(5*H*)-one in a basic medium using freshly prepared fused sodium acetate to produce the target 5–(7-fluoro-11*H*-indeno[1,2-*b*]quinoxalin-11-ylidene)-2-hydrazineylthiazol-4(5*H*)-one (**10**), Scheme 3. Elemental analysis and spectrum data proved the product. Along with a carbonyl band at 1711 cm^{-1}, IR spectra showed NH_2 and NH bands at 3415 and 3190 cm^{-1}. Aside from two signals that emerged at δ 5.43 and 7.89 ppm due to NH_2 and NH, ^{1}H NMR also showed signals caused by aromatic protons. In addition to signals for the aromatic carbons, its ^{13}C NMR provided signals at δ 172.16 for the carbonyl group, 161.58 ppm for carbon attached to fluoride atom, δ 158.91 for (S-C=N), and 157.13 ppm for (C=N) groups. Also as viewed in Scheme 3, the two reagents **11a** and **11b** were prepared according to previous work [51,52], and allowed to react with the starting material **3** in a basic medium using freshly prepared fused sodium acetate to produce the corresponding **12** and **13**. The structure of **12** was confirmed by microanalyses and spectral data. The IR spectrum exhibited a band at 3422 cm^{-1} related to the NH group in addition to the carbonyl band at 1729 cm^{-1}. The ^{1}H NMR spectrum of the same compound showed the exchangeable signal of the NH group at δ 8.90 ppm and the signals for seventeen aromatic protons. Furthermore, its ^{13}C NMR indicated three signals at δ 164.99, 172.31, and 174.44 ppm for S-C=N, C-F, and C=O groups, besides the aromatic carbons. Also, the ^{1}H NMR spectrum of compound **13** elicited two singlet signals at δ 10.67 and 11.05 ppm attributed to 2NH protons, besides the signals associated with the aromatic Hs. Additionally, ^{13}C NMR presented signals between δ 110.29 to 157.24 ppm, and four signals at δ 164.97, 168.86, 171.92, and 171.97 ppm related to (S-C=N), (C-F), and (2C=O) groups correspondingly.

Thiosemicarbazone derivatives are very useful and widely used as a synthetic initial compound for thiazole synthesis. Consequently, compound **3** was allowed to react with thiosemicarbazide to produce the corresponding thiosemicarbazone derivative **14**, Scheme 4. Its IR spectrum doesn't have the C=O group absorption band present in compound **3** and at the same time revealed NH_2 and NH group absorption bands at 3448, 3396, and 3275 cm^{-1} respectively. The ^{1}H NMR spectrum exhibited two singlet signals at δ 8.15, and 12.48 ppm relevant to the NH_2, and NH protons together with signals related to the aromatic protons. Furthermore, thiosemicarbazone derivative **14** was cyclo-alkylated to obtain many biologically active thiazole compounds. Thus, the interaction of compound **14** with an alkylating agent (ethyl 2-chloropropanoate, ethyl

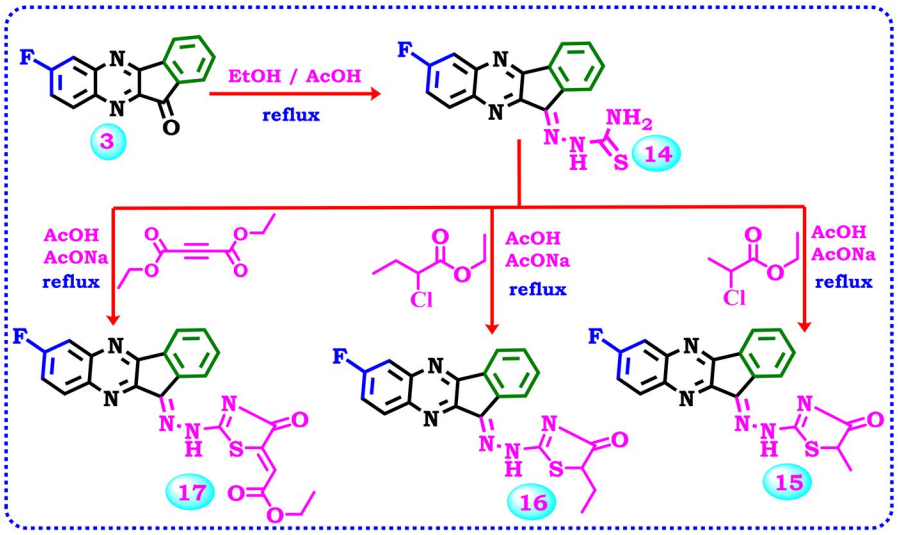

Scheme 4. Synthesis of thiosemicarbazone derivative **14** and its cyclisation to afford the thiazole derivatives **15–17**.

2-chlorobutanoate) or diethyl but-2-ynedioate produced the corresponding different derivatives **15–17**, Scheme 4. The IR spectrum of compound **15** exhibited bands at 3396 cm^{-1} for the NH_2 group, and 1722 cm^{-1} due to the C=O group. The ^1H NMR field confirmed its structure through the appearance of a singlet signal at δ 1.45 ppm corresponding to the hydrogens of the methyl, a quartette signal at δ 3.81 ppm representing CH of thiazolone, signals in the region δ 7.54–8.26 ppm showing the aromatic protons, in addition to singlet signal at δ 8.84 ppm due to NH group. While the ^1H NMR spectrum of **16** displayed a triplet signal at δ 0.99 due to ($\underline{CH_3}$-CH_2), a signal at δ 2.02 ppm corresponding to (CH_3-$\underline{CH_2}$), triplet signal at δ 4.33 assignable to the CH in the thiazole, and a singlet signal at δ 12.64 for the NH group beside the signals of the aromatic protons. The ^{13}C NMR spectrum showed the presence of two aliphatic carbons at δ 19.85, and 57.87 ppm, whereas the carbon attached to the flour and the carbonyl carbon were observed at δ 154.29, and 178.79 ppm respectively. Finally, The IR spectrum of thiazolone derivative **17** displayed absorption bands at 3263, 1727, and 1700 cm^{-1} related to NH, and two carbonyl groups respectively. Also, its ^1H NMR spectrum revealed two signals at δ 1.27, and 4.24 ppm due to the ethyl group, besides a signal at δ 6.64 ppm for the CH-vinilic, and a signal at δ 7.98 ppm for the NH group, in addition to the aromatic protons. ^{13}C NMR spectrum was characterised by signals at δ 14.57, 61.55, and 96.97 ppm representing the two aliphatic carbons of the ethyl group, and CH-vinylic, as well as signals at δ 158.28, 161.62, 165.01 ppm related to (C=N), (S-C=N), (C-F) carbons, and two signals at δ 166.24, 166.38 ppm assignable to (2C=O) groups besides signals in the aromatic region owing to the aromatic carbons.

Biology

Blood glucose and plasma insulin level

Streptozotocin (STZ) causes a significant increase in blood sugar and a big drop in insulin levels in the plasma. When gliclazide and the newly synthesised hybrids were used, blood sugar levels declined significantly, and insulin levels rose compared to the STZ-only treatment group ($p<0.05$) (Table 1).

Kidney function parameters

STZ resulted in a nephropathy state manifested by a significant elevation of plasma urea and creatinine levels as compared to normal control mice. Treatment with gliclazide and **4**, **6**, **8**, and **16** led to a significant lowering in plasma urea and creatinine levels as related to STZ only treated group $p<0.05$ (Table 2).

Oxidative stress markers

A biomarker for oxidative stress (MDA) was significantly higher in the diabetes group that wasn't treated. Along with this, there was a big drop in plasma antioxidant (GSH). Treatment with gliclazide and hybrids **4**, **6**, **8**, and **16** demonstrated a significant reduction of oxidative stress marker (MDA) and significant elevation in GSH as compared to the diabetic non-treated group, $p<0.05$ (Table 2).

Liver function markers and cholesterol

The administration of STZ led to the deterioration of liver function biomarkers, as evidenced by a notable increase in AST and ALT levels. In addition to a significant elevation in total cholesterol, $p<0.05$ (Table 2). Treatment of the diabetic group with gliclazide or hybrids **4**, **6**, **8**, and **16** for 2 weeks resulted in a significant reduction of TC and liver function tests (AST and ALT), $p<0.05$ (Table 2).

α-Glucosidase inhibition assay

The brush border of the small intestine contains the enzyme α-glucosidase, which controls the enzymatic hydrolysis of 1,4-linked polysaccharides with glucose as one of the main byproducts. Glucosidase is a target for the treatment of postprandial hyperglycaemia because of the significant role that glucose plays as one of the primary sources of energy in eukaryotes. The anti-diabetic medication acarbose belongs to a group of medications called α-glucosidase inhibitors (AGIs), which stop the gastrointestinal tract from absorbing glucose. In vitro α-glucosidase inhibitory activity of the target hybrids **4**, **6**, **8**, and **16** was assessed in relation to the reference medication acarbose (IC_{50}= 0.316±0.02 μM). Table 3 provided a summary of the findings. Both substances were discovered to be strong inhibitors of the α-glucosidase enzyme, as shown below. However, the hydrazone derivative (1–(2-(2–(7-fluoro-11*H*-indeno[1,2-*b*]quinoxalin-11-ylidene)-hydrazineyl)-4-methyl-thiazol-5-yl)-ethan-1-one) (**8**) was found to be more active as α-glucosidase inhibitory activity with IC_{50} value of 0.982±0.04 μM, followed by Schiff base derivative **6** with IC_{50} 2.995±0.09 μM. Additionally, the hydrazone derivative **16** has good activity as an inhibitor of α-glucosidase,

Table 1. Effect of two weeks of treatment with new hybrids **4–17** as well as Gliclazide on plasma glucose and insulin level in STZ-induced diabetes in mice.

Parameters Groups	Glucose 3rd day (mg/dL)	Glucose 6th day	Glucose 9th day	Glucose 12th day	Glucose 15th day	Insulin (ng/mL)
NC	98.67 ± 4.4[b]	98.67 ± 4.4[b]	98.67 ± 4.4[b]	98.67 ± 4.4[b]	98.67 ± 4.4[b]	16.75 ± 0.5[b,c]
PC	279.17 ± 10.2[a]	357.50 ± 18.96[a]	540 ± 26.6[a,c]	519.17 ± 27.8[a,c]	486.67 ± 11.4[a,c]	3.14 ± 0.2[a,c]
Gliclazide	358.33 ± 18.1[a]	199.67 ± 5.8	165 ± 4.1[b]	132.33 ± 3.7[b]	118.33 ± 3.3[b]	14.52 ± 0.4[a,b]
4	311.33 ± 19.5[a]	293.33 ± 17.8[a]	304.17 ± 7.1[a,b]	187 ± 3.4[b]	162.83 ± 1.8 b	11.44 ± 0.2[a,b]
5	436.67 ± 51.6[a]	566.67 ± 15.4[a,b,c]	251.67 ± 13.5[b]	300 ± 18.2[a,b]	256.67 ± 19.9[a,b]	
6	332.50 ± 18.4[a]	363.83 ± 69[a]	220 ± 13.9[b]	177.50 ± 3.8[b]	155.67 ± 3.6[b]	12.28 ± 0.3[a,b]
7	478.33 ± 44.7[a,b]	543.33 ± 17.6[a,c]	280.83 ± 27.5[a,b]	230 ± 9.3[b]	216.67 ± 10.6[b]	
8	313.33 ± 4.9[a]	238.33 ± 4.8	202.50 ± 3.6[b]	214.83 ± 9.97[b]	175 ± 11.5[b]	10.5 ± 0.3[a,b]
9	321.67 ± 35.5[a]	300.83 ± 34.7[a]	275.17 ± 24[a,b]	355 ± 18.4[a,c]	337.17 ± 11.4[a,c]	
10	385.83 ± 61.2[a]	381.67 ± 23.3[a]	305.33 ± 16.4[a,b]	408.33 ± 40.3[a,c]	368.33 ± 33[a,c]	
12	343.00 ± 52.8[a]	288.33 ± 77.9	332.17 ± 79.1[a,b]	251.67 ± 60.8[b]	325 ± 15.6[a,b,c]	
13	340.83 ± 39.2[a]	240 ± 54.2	295 ± 80.3[a,b]	226.67 ± 48.6[b]	225 ± 46.7[b]	
14	351.67 ± 16.6[a]	258.33 ± 16.6	213 ± 10.3[b]	387.50 ± 82.7[a,c]	320.50 ± 79.9[a,b,c]	
15	321.67 ± 24.7[a]	356.67 ± 29.6[a]	294.17 ± 31.3[a,b]	318.33 ± 27.7[a,b,c]	294.17 ± 31.3[a,b,c]	
16	313.33 ± 23.8[a]	254.50 ± 9.7	217.50 ± 6.3[b]	202 ± 13.5[b]	169 ± 1.5[b]	9.34 ± 0.3[a,b]
17	410 ± 57.6[a]	350.83 ± 80[a]	294.17 ± 60.9[a,b]	323.33 ± 65.2[a,b,c]	312.50 ± 63[a,b,c]	

Each value represents the mean of 6 mice ± SEM. Statistical analysis was carried out using one-way analysis of variance (ANOVA) followed by Tukey Kramer multiple comparisons test.
[a]significantly different from normal control (NC) ($p < 0.05$)
[b]significantly different from positive control (PC) ($p < 0.05$)
[c]significantly different from standard ($p < 0.05$).

Table 2. Effect of two weeks of treatment with **4**, **6**, **8**, and **16** on plasma levels of urea, creatinine, GSH, MDA, ALT, AST, and total cholesterol in STZ-induced diabetes in mice.

Parameter Groups	Urea	Creat	GSH	MDA	ALT	AST	TC
NC	55.1 ± 0.3	2.03 ± 0.1	4.56 ± 0.02	18.57 ± 0.2	44.4 ± 0.8	35.2 ± 0.3	65.3 ± 0.4
PC	91.6 ± 0.5[a]	7.8 ± 0.1[a]	0.998 ± 0.04[a]	40.3 ± 0.8[a]	96.7 ± 0.7[a]	87.6 ± 0.7[a]	150.3 ± 1[a]
Gliclazide	57.5 ± 0.3[a,b]	3.3 ± 0.1[a,b]	3.15 ± 0.05[a,b]	22 ± 0.2[a,b]	53.7 ± 0.7[a,b]	39.8 ± 0.3[a,b]	74.4 ± 0.6[a,b]
4	60.5 ± 0.4[a,b]	5.1 ± 0.1[a,b]	2.17 ± 0.03[a,b]	23.9 ± 0.2[a,b]	66 ± 0.4[a,b]	46.4 ± 0.2[a,b]	79.3 ± 0.4[a,b]
6	59.5 ± 0.2[a,b]	4.9 ± 0.1[a,b]	2.5 ± 0.02[a,b]	22.9 ± 0.3[a,b]	59.6 ± 0.2[a,b]	46.1 ± 0.3[a,b]	77.5 ± 0.5[a,b]
8	63.2 ± 0.3[a,b]	5.9 ± 0.1[a,b]	1.72 ± 0.03[a,b]	27.7 ± 0.3[a,b]	72.5 ± 0.9[a,b]	54.2 ± 0.4[a,b]	86.3 ± 0.7[a,b]
16	62 ± 0.3[a,b]	5.5 ± 0.1[a,b]	1.99 ± 0.03[a,b]	24.9 ± 0.2[a,b]	68.2 ± 0.6[a,b]	47.6 ± 0.2 [a,b]	81.5 ± 0.3[a,b]

Each value represents the mean of 6 mice ± SEM. Statistical analysis was carried out using one-way analysis of variance (ANOVA) followed by Tukey Kramer multiple comparisons test.
[a]significantly different from normal control (NC) ($p < 0.05$)
[b]significantly different from positive control (PC) ($p < 0.05$)
[c]significantly different from standard ($p < 0.05$).

Table 3. Effects of indenoquinoxaline-containing thiazole analogs **4**, **6**, **8**, and **16** as well as acarbose on *α*-glucosidase activity.

Ser.	Cpd. No.	*α*-Glucosidase IC_{50} (μm)	DF = 100 ± SD
1	4	10.19	0.21
2	6	2.995	0.09
3	8	0.982	0.04
4	16	7.029	0.13
Standard	Acarbose	0.316	0.02

Results represent IC_{50} (Half maximal inhibitory concentration) of indenoquinoxaline-containing thiazole analogs ± SD as compared to acarbose on *α*-glucosidase activity.

Table 4. Effects of indenoquinoxaline-containing thiazole analogs **4**, **6**, **8**, and **16** as well as acarbose on *α*-amylase activity.

Ser.	Cpd. No.	*α*- Amylase IC_{50} (μM)	DF = 10 ±SD
1	4	93.36	3.95
2	6	32.29	1.37
3	8	17.58	0.74
4	16	121.6	5.14
Standard	Acarbose	31.56	1.33

Results represent IC_{50} (Half maximal inhibitory concentration) of indenoquinoxaline-containing thiazole analogs ± SD as compared to acarbose on *α*-amylase activity.

which suggests that the most potent hybrids are those that contain indenoquinoxalene and thiazole connected with hydrazone, followed by Schiff base linker.

Table 5. Physicochemical properties according to TPSA, and % ABS.

Cpd. No.	TPSA[a]	% ABS[b]
4	92.87	76.96
5	96.34	75.76
6	105.57	72.58
7	104.9	72.81
8	108.37	71.61
9	117.6	68.43
10	118.56	68.1
12	122.72	66.66
13	134	62.77
14	108.28	71.64
15	104.9	72.81
16	104.9	72.81
17	131.2	63.74
Acarbose	321.17	−1.8
Gliclazide	86.89	79.02

[a]topological polar surface area ($Å^2$)
[b]% absorption

α-Amylase inhibition assay

Changes to *α*-amylase activity have an impact on the utilisation of carbohydrates as a fuel source. This enzyme is necessary for the digestion of complex carbohydrates in humans. Inhibition of *α*-amylase is seen as a possible target for the treatment of diseases like diabetes, obesity, dental caries, and periodontal problems that are linked to carbohydrate intake. *In vitro α*-amylase inhibitory activity of compounds **4**, **6**, **8**, and **16** was assessed in relation to the reference medication acarbose (IC_{50} =

31.56 ± 1.33 μM). Table 4 provided a summary of the findings. All the substances examined were discovered to be strong inhibitors of the α-amylase enzyme. Particularly, Schiff base derivative **6** and hydrazone derivative **8** show that these moieties are crucial for the anti-diabetic effects.

Table 6. Physicochemical properties of the newly synthesised hits.

Cpd. No.	Fraction Csp3[a]	No. of Rotatable bonds	HBA[b]	HBD[c]	iLOGP[d]	MR[e]
4	0.06	1	6	0	2.59	98.74
5	0.1	2	6	0	3.39	107.51
6	0.14	4	7	0	3.83	113.4
7	0.06	2	6	1	2.32	101.54
8	0.1	3	6	1	2.98	111.29
9	0.14	5	7	1	3.43	117.18
10	0	1	6	2	2.34	100.88
12	0.03	5	7	1	4.37	178.67
13	0	2	7	2	4.37	141.48
14	0	2	4	2	2.58	89.74
15	0.11	2	6	1	2.82	106.35
16	0.15	3	6	1	2.74	111.15
17	0.09	5	8	1	2.74	121.58
Acarbose	0.92	9	19	14	0.63	136.69
Gliclazide	0.53	5	4	2	1.96	86.93

[a]The ratio of sp^3 hybridised carbons over the total carbon count of the molecule
[b]number of hydrogen bond acceptors
[c]number of hydrogen bond donors
[d]lipophilicity; [e]Molar refractivity.

In silico studies

In silico assessment of physicochemical and ADME properties

The compounds' physicochemical parameters, lipophilicity, water-solubility, pharmacokinetics, drug-likeness, medicinal chemistry properties, and bioavailability score were calculated using SwissADME (http://www.swissadme.ch). Bioavailability is a quick assessment of substances to determine their suitability as an oral medication.

Using SwissADME, the physicochemical and ADME properties of the newly made thiazole-containing compounds **4**, **5**, **6**, **7**, **8**, **9**, **10**, **12**, **13**, **14**, **15**, **16**, and **17**, as well as **acarbose** and **gliclazide** were studied (Table 5).

Topological polar surface area (TPSA) (Table 5) values for all drugs are less than 140 A0, indicating high oral bioavailability. The estimated% ABS shows that all hits ranged between percentages of ABS were computed using the formula % ABS = 109 –(0.345 ×TPSA).

Rotatable bonds in all compounds are between 1 and 5, which suggests that the molecule is flexible concerning its bio target. Also, all compounds have hydrogen bond acceptor (HBA) sites less than 10. They also have less than 5 for hydrogen bond donor (HBD) sites. Additionally, Molar refractivity was from 40 to 130 for all compounds except compounds **12** and **13** (Table 6).

Table 7 for the drug similarity predictor demonstrates that all synthesised compounds meet Lipinski's requirements for oral medications, except for compounds **12** and **13**, which have just one infraction. While occasionally inadequate absorption can result from violating even one of these rules. A common method for

Table 7. Bioavailability and drug-likeness predictions of substances 4–17 in addition to Acarbose and Gliclazide.

Cpd. No.	Lipinski (violations)	Veber (violations)	Ghose (violations)	Egan (violations)	Muegge (violations)	Bioavailability Score	PAINS alerts	Synthetic Accessibility
4	0	0	0	0	0	0.55	0	3.44
5	0	0	0	0	0	0.55	0	3.54
6	0	0	0	0	0	0.55	0	3.7
7	0	0	0	0	0	0.55	0	3.43
8	0	0	0	0	0	0.55	0	3.56
9	0	0	0	0	1	0.55	0	3.75
10	0	0	0	0	0	0.55	1	3.66
12	1	0	3	1	3	0.55	1	4.78
13	1	0	3	1	3	0.55	1	4.78
14	0	0	0	0	0	0.55	0	3.03
15	0	0	0	0	0	0.55	0	3.99
16	0	0	0	0	0	0.55	0	4.09
17	0	0	0	0	0	0.55	0	4.09
Acarbose	3	1	4	1	5	0.17	0	7.34
Gliclazide	0	0	0	0	0	0.55	0	3.52

Table 8. Pharmacokinetic/ADME properties of the tested novel compounds.

Cpd. No.	GI absorption	BBB permeant	Pgp substrate	CYP1A2 inhibitor	CYP2C19 inhibitor	CYP2C9 inhibitor	CYP2D6 inhibitor	CYP3A4 inhibitor
4	High	No	No	Yes	Yes	Yes	No	Yes
5	High	No	No	Yes	Yes	Yes	No	Yes
6	High	No	No	Yes	Yes	Yes	No	Yes
7	High	No	No	Yes	Yes	Yes	No	Yes
8	High	No	No	Yes	Yes	Yes	No	Yes
9	Low	No	No	No	Yes	Yes	No	Yes
10	High	No	No	Yes	No	No	No	Yes
12	Low	No	No	No	No	No	No	No
13	Low	No	No	No	No	No	No	No
14	High	No	No	Yes	No	Yes	No	Yes
15	High	No	No	Yes	Yes	Yes	No	Yes
16	High	No	No	Yes	Yes	Yes	No	Yes
17	High	No	No	Yes	Yes	Yes	No	Yes
Acarbose	Low	No	Yes	No	No	No	No	No
Gliclazide	High	No	Yes	No	No	No	No	No

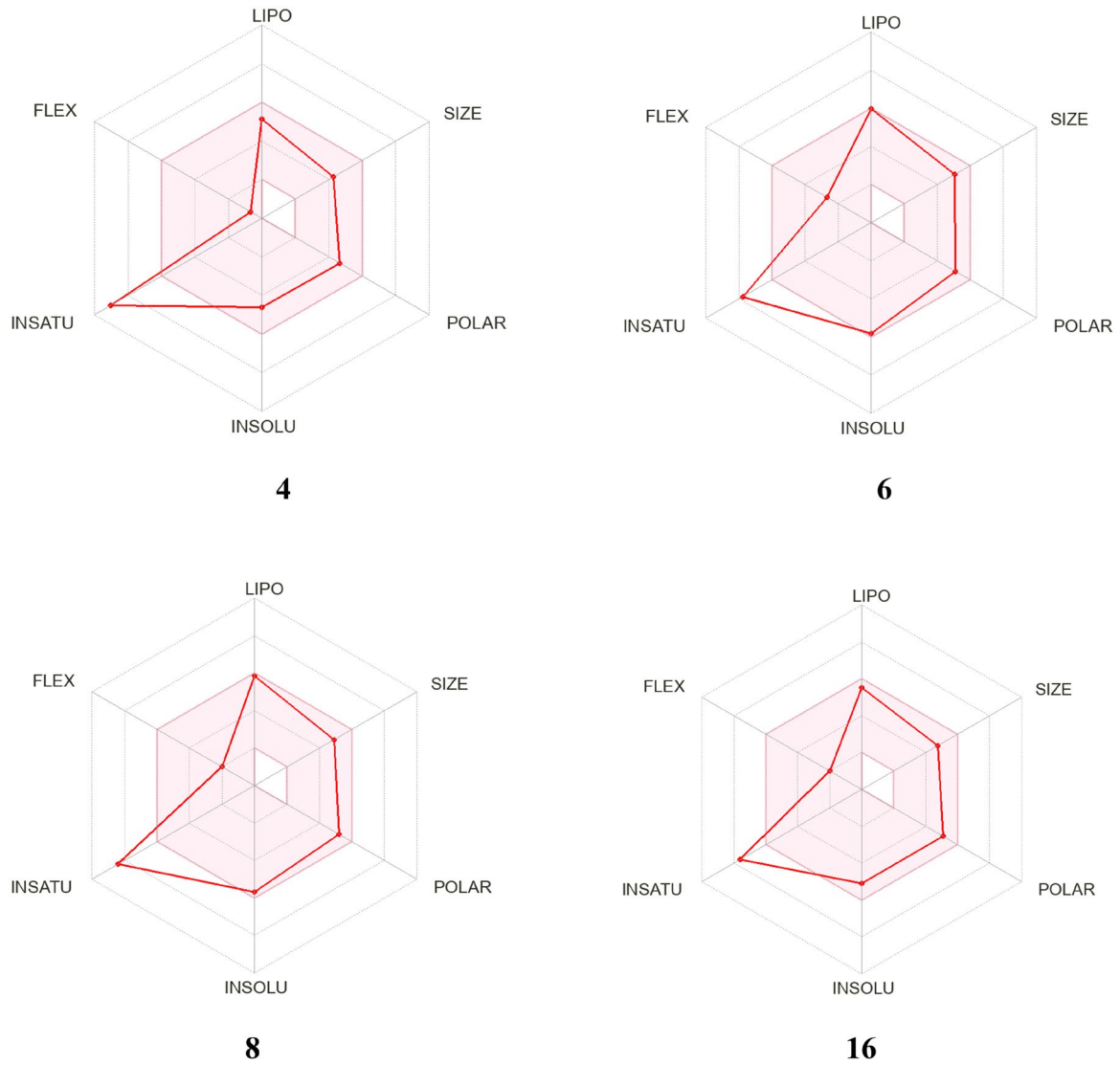

Figure 2. Diagrams showing how compounds **4**, **6**, **8**, and **16** correlate to drugs. The coloured area is a good physical and chemical space for oral bioavailability. LIPO (lipophilicity); SIZE (molecular weight); POLAR (polarity); INSOLU (insolubility); INSATU (insaturation); FLEX (flexibility).

Table 9. Toxicity of the most promising hits compared to acarbose and gliclazide.

Cpd. No.	AMES toxicity	Max. tolerated dose (human) (log mg/kg/day)	hERG I inhibitor	hERG II inhibitor	Oral Rat Acute Toxicity (LD_{50}) (mol/kg)	Oral Rat Chronic Toxicity (LOAEL) (log mg/kg_bw/day)
4	Yes	−0.409	No	No	2.682	0.862
6	No	0.187	No	Yes	2.672	0.733
8	No	0.093	No	Yes	2.816	0.74
16	No	−0.204	No	Yes	2.505	0.745
Acarbose	No	0.616	No	Yes	3.176	7.01
Gliclazide	No	−0.04	No	No	1.932	1.745

Table 10. Continuation of toxicity of the most promising hits compared to acarbose and gliclazide.

Cpd. No.	Hepatotoxicity	Skin Sensitisation	*T.Pyriformis* toxicity (log ug/L)	Minnow toxicity (log mM)
4	Yes	No	0.413	0.321
6	Yes	No	0.287	0.729
8	Yes	No	0.294	0.605
16	Yes	No	0.385	−0.905
Acarbose	No	No	0.285	15.114
Gliclazide	Yes	No	1.038	0.659

Table 11. Toxicity prediction with ProTox-II website for the most active derivatives compared to acarbose and gliclazide.

Cpd. No.	LD_{50} (mg/kg)	Toxicity Class	Carcinogenicity Prediction (Probability)	Immunotoxicity Prediction (Probability)	Mutagenicity Prediction (Probability)	Cytotoxicity Prediction (Probability)
4	2000	4	Inactive (0.54)	Inactive (0.94)	Inactive (0.58)	Inactive (0.72)
6	300	3	Inactive (0.51)	Inactive (0.97)	Inactive (0.68)	Inactive (0.68)
8	807	4	Inactive (0.53)	Inactive (0.96)	Active (0.58)	Inactive (0.75)
16	2000	4	Active (0.5)	Active (0.59)	Active (0.52)	Inactive (0.77)
Acarbose	24000	6	Inactive (0.84)	Active (0.99)	Inactive (0.76)	Inactive (0.70)
Gliclazide	1750	4	Inactive (0.79)	Inactive (0.99)	Inactive (0.79)	Inactive (0.66)

assessing a compound's drug-likeness is Lipinski's rule of five. A drug-like compound should meet no more than one of the following requirements, according to Lipinski's rule: 'a molecular weight of less than 500 g/mol, a log *p* values of less than 5, no more than five hydrogen bond donors (HBD), and no more than 10 hydrogen bond acceptor (HBA) sites.' Based on the screening method that follows Veber's guidelines, all the hits pass the test for drug resemblance.

Table 12. Binding energies S (Kcal mol^{-1}), receptor interactions and distances in angstroms of acarbose, with α-amylase (PDB ID: 1B2Y) and α-glucosidase (PDB ID: 5NN8) (London dG as a scoring function).

Ligand/ Protein	Receptor Amino Acid names and number	Type of interaction	Distance (Å)
α-Amylase	GLU 240	H-donor	2.78
	HIS 201	H-donor	2.67
	GLU 233	H-donor	2.58
	GLU 233	H-donor	2.63
	ASP 300	H-donor	3.03
	GLU 233	H-donor	3.26
	ASP 300	H-donor	2.54
	ASP 197	H-donor	3.37
	ASP 197	H-donor	2.7
	ASP 300	H-donor	3.18
	TRP 59	H-donor	2.69
	THR 163	H-donor	2.8
	LYS 200	H-acceptor	2.77
	ARG 195	H-acceptor	2.91
	HIS 299	H-acceptor	3.06
	HIS 299	H-acceptor	3.37
	HIS 305	H-acceptor	2.76
	GLN 63	H-acceptor	2.86
	TYR 151	H-pi	4.59
	TRP 59	H-pi	4.47
	TRP 59	H-pi	3.92
α-Glucosidase	ASP 282	H-donor	2.77
	ASP 282	H-donor	2.65
	MET 519	H-donor	3.18
	ASP 616	H-donor	3.24
	MET 519	H-donor	4.32
	ASP 616	H-donor	2.55
	ASP 404	H-donor	2.65
	ASP 404	H-donor	2.54
	ARG 600	H-acceptor	2.64
	HIS 674	H-acceptor	2.87
	PHE 649	H-pi	4.28

The Ghose, Egan, and Muegge guidelines say that all derivatives except compounds **12** and **13** follow the rule and could be used as medicines. Also, Muegge rules are broken in compound **9**. All compounds that were looked at, had a score of 0.55 for bioavailability which is a high score.

(PAINS), which was made by SwissADME, showed no alerts for all hits except **10**, **12**, and **13**. Those three only had one alert. Even though PAINS are important features to consider when making drugs to avoid false positives, overestimating them, and using them blindly could mean that promising hits are left out because of fake PAINS. All the analogs were given scores between 3.43 and 4.78 for how easy they are to produce, which means that they can be made in large quantities (Table 7).

Regarding the pharmacokinetic and medicinal chemistry aspects of the produced compounds (Table 8), it was determined that all derivatives have high gastrointestinal absorption, except compounds **9**, **12**, and **13**. All of them can't get through the blood-brain barrier. This means that these molecules that are targeted to the whole body will have few or no effects on the CNS. The investigation of the P-glycoprotein (P-gp) non-substrate candidature was another key issue throughout the preclinical analysis trial. Pgp functions as an efflux transporter, pumping medicines, other substances, and its substrate out of the cell (Figure 2).

As a result, the hits were examined using the SwissADME website. We discovered that all the hits are not P-gp protein substrates, as shown in (Table 8), implying that these hits have a minimal probability of efflux out of the cell.

The metabolic profile obtained (Table 8) revealed that all the screened derivatives, except for compounds **9**, **12**, and **13**, are inhibitors of the CYP1A2 enzyme, in addition to acarbose and gliclazide. Except for **10**, **12**, **13**, **14**, **acarbose**, and **gliclazide**, all are also CYP2C19 inhibitors. Compounds **10**, **12**, **13**, **acarbose**, and **gliclazide** are not CYP2C9 inhibitors or substrates. All the hits are not CYP2D6 substrates. All drugs inhibit CYP3A4 except **12**, **13**, **acarbose**, and **gliclazide**.

Toxicity prediction

Safety is always crucial to consider while developing a new drug. Safety encompasses a variety of toxicities and unfavourable

Table 13. Binding energies S (Kcal mol^{-1}), receptor interactions, and distances in angstroms of compounds **4**, **6**, **8**, and **16**, with α-amylase (PDB ID: 1B2Y) and α-glucosidase (PDB ID: 5NN8) (London dG as a scoring function).

Compound	Binding Energy (*S*) (kCal/mol)	Receptor Amino Acid	Type of interaction	Distance (Å)	Binding Energy (*S*) (kCal/mol)	Receptor Amino Acid	Type of interaction	Distance (Å)
	1B2Y				5NN8			
4	−7.93	GLY 306	pi-H	3.81	−7.83	HIS 674	H-acceptor	3.38
6	−9.72	HIS 201	H-donor	3.6	−10.63	ASP 616	H-donor	3.53
		HIS 305	H-acceptor	3		ASP 645	H-donor	3.15
		LYS 200	H-acceptor	2.85		TRP 481	H-acceptor	3.2
		HIS 305	pi-H	4.49		HIS 674	H-acceptor	3.38
		GLY 306	pi-H	4.01				
		GLY 306	pi-H	4.61				
8	−11.59	GLU 233	H-donor	3.3	−10.79	ASP 616	H-donor	3.39
		LYS 200	H-acceptor	2.9		ASP 616	H-donor	3.22
		HIS 101	H-pi	4.84		TRP 481	H-acceptor	3.25
						HIS 674	H-acceptor	2.95
						LEU 283	pi-H	4.57
16	−7.37	GLN 63	H-acceptor	3.39	−9.37	ASP 616	H-donor	3.37
		TRP 59	H-pi	4.34		ASP 616	H-donor	3.44
		TRP 59	H-pi	3.88		TRP 481	H-acceptor	3.18
		LEU 162	pi-H	4.02		LEU 83	pi-H	4.6
		LEU 162	pi-H	4.23				

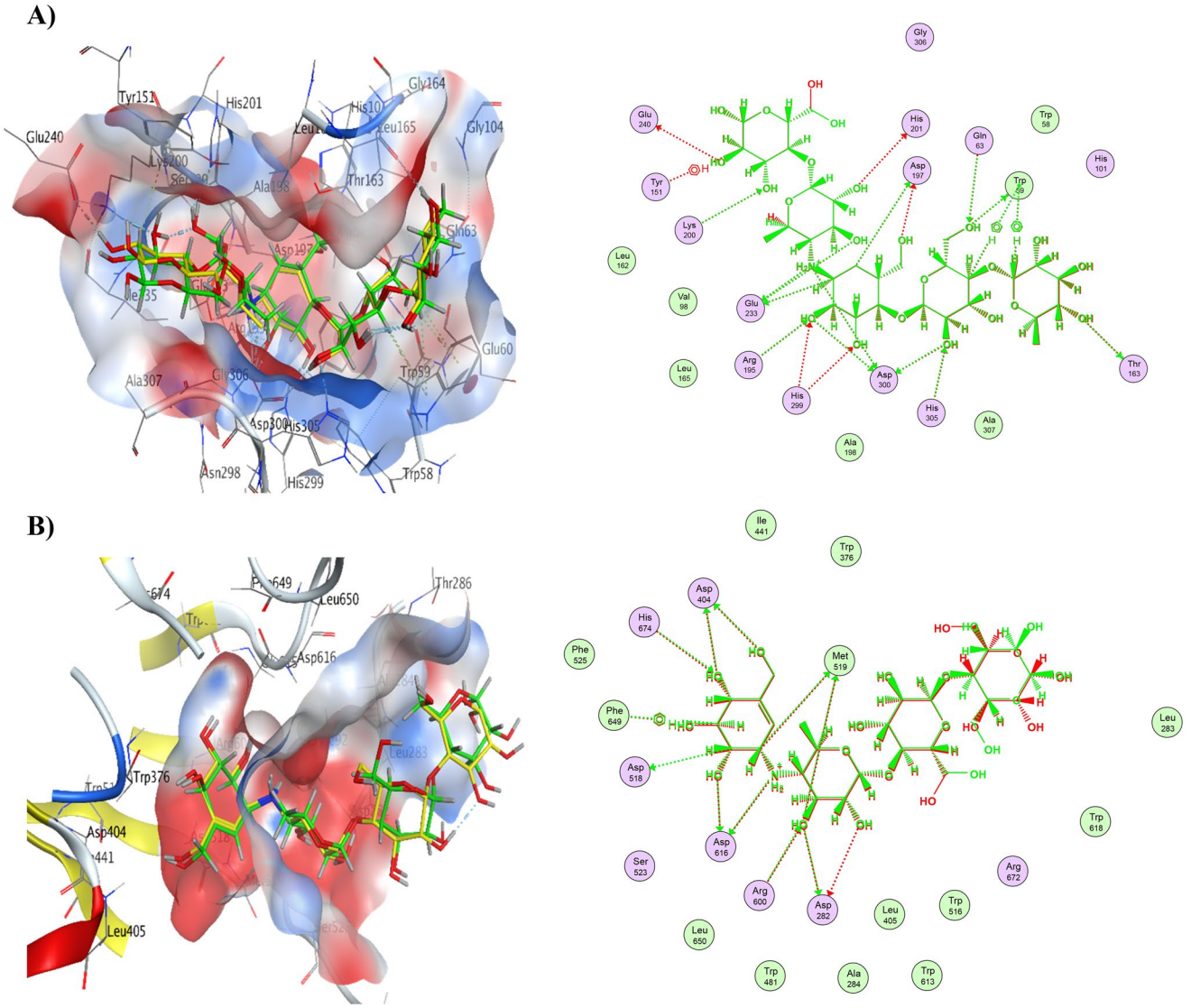

Figure 3. A) Overlay between co-crystallized ligand (yellow) and re-docked pose (green) of acarbose (RMSD= 0.66 Å) in *α*-amylase (PDB ID: 1B2Y), complex overlay and ligand interactions. B) Overlay between co-crystallized ligand (yellow) and re-docked pose (green) of acarbose (RMSD= 0.56 Å) in *α*-glucosidase (PDB ID: 5NN8), complex overlay and ligand interactions.

adverse effects that should be investigated during the drug development journey.

In this work, we investigate the toxicity of the most promising compounds **4**, **6**, **8**, and **24** besides two antidiabetic drugs **(acarbose** and **gliclazide)** with the aid of the ProTox-II website (https://tox-new.charite.de/protox_II), and pkCSM website (http://biosig.unimelb.edu.au/pkcsm/prediction), and the results were shown in Tables 9, 10, and 11.

Except for compound **4**, none of the compounds in Table 9 including **acarbose** and **gliclazide** exhibited AMES toxicity in the pkCSM web tools. The maximum acceptable human dose for the components that are the most bioactive ranges from −0.409 to 0.616 log mg/kg/day. Additionally, it was discovered that none of the tested substances inhibit hERG I, which is a positive finding that makes the substances safer and lowers the risk factors for torsade de pointes (a deadly arrhythmia). Contrarily, the only compounds that do not block hERG II are compound **4** and gliclazide. Gliclazide's acute oral rat toxicity values ranged from 1.932 mol/kg to 3.176 mol/kg, whereas acarbose's acute oral rat toxicity (LOAEL) values ranged from 0.737 to 7.01 log mg/kg_ bw/day.

Hepatotoxicity is a rare reason for drug development to halt during the preclinical stage. In fact, liver toxicity is typically reversible in contrast to other organ toxicity, and sensitive serum enzyme assays can be used to monitor liver toxicity in humans. To confirm whether a substance is also hepatotoxic in humans, it is frequently tested on humans after it was discovered to be hepatotoxic in an animal species. In our investigation, gliclazide and all other evaluated substances are anticipated to be hepatotoxic. Hepatotoxicity was absent in just acarbose. However, none of the hits revealed any signs of cutaneous sensitivity. *Tetrahymena pyriformis's* toxicity ranges from 0.285 to 1.038, making it a common indicator of toxicity endpoints.

As shown in (Table 11), the toxicity profile for the active chemicals **4**, **6**, and **gliclazide** demonstrated that they were not mutagenic, immune-toxic, carcinogenic, or cytotoxic, with LD_{50} values of 2000, 300, and 1750, respectively. Compound **8** was projected to be non-carcinogenic, non-immunogenic, and non-cytotoxic but active for mutagenicity, with an LD_{50} of 807 mg/kg. Furthermore, compound **16** was noncytotoxic, but it was mutagenic, immune-toxic, and carcinogenic in toxicity experiments, with an LD_{50} of 2000 mg/kg. Acarbose

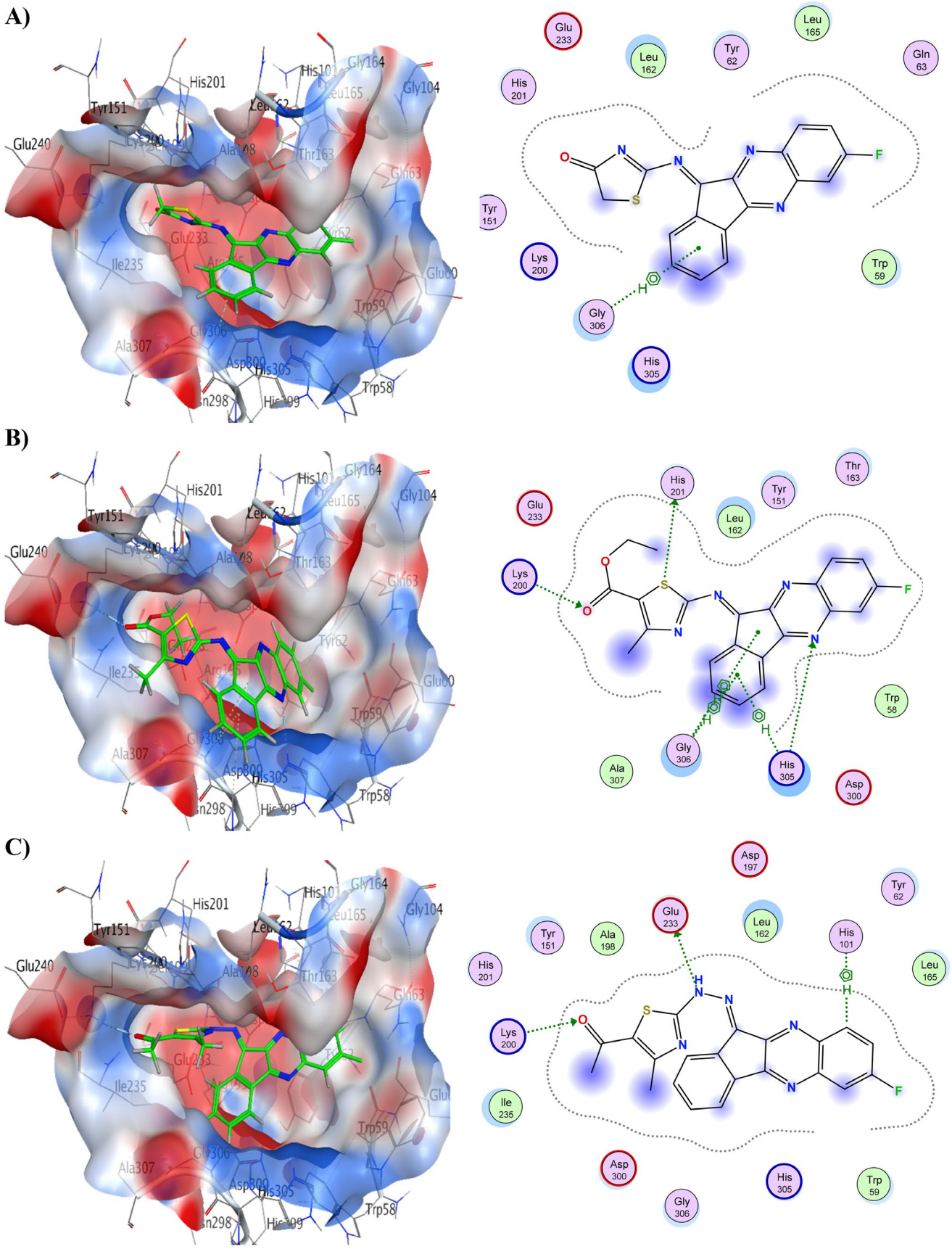

Figure 4. 3D binding modes & 2D ligand interactions with α-amylase (PDB ID: 1B2Y) of the most active compounds, (A) Compound **4**, (B) Compound **6**, (C) Compound **8**, (D) Compound **16**.

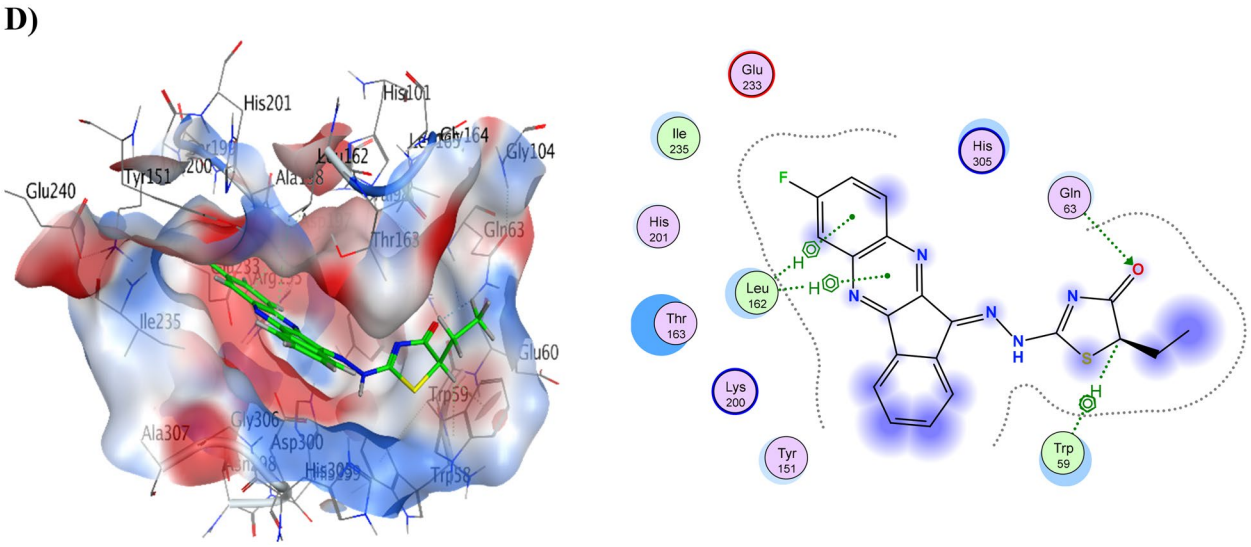

Figure 4. Continued.

was also discovered to be immunogenic but not carcinogenic, mutagenic, or cytotoxic. Furthermore, the novel-generated quinoxaline derivatives **4**, **8**, and **16** were classified as class four toxicity, whereas derivative **6** was classified as class three toxicity.

Docking studies

To verify the accuracy of the docking procedure used in this docking investigation, self-docking of the co-crystalized ligand (acarbose) in the binding site was performed for *α*-amylase and α-glucosidase. The low RMSD between acarbose's re-docked stance and native pose served as proof that the validation stage was successful. The RMSD for self-docking of *α*-amylase (PDB ID: 1B2Y) was 0.6608 Å. The RMSD value for self-docking of *α*-glucosidase (PDB ID: 5NN8) was 0.5693 Å. Additionally, as shown in Figure 3, the re-docked acarbose pose in both proteins demonstrated the capacity to overlap the native ligand posture and occupy important contacts made possible by the co-crystallized ligand with the active site hot spots in *α*-amylase and *α*-glucosidase (Table 12).

Compounds **6** and **8** showed the lowest energy in the case of *α*-amylase, with score values of −9.72 and −11.59 kCal/mol, respectively. This demonstrates that it agrees with the findings of the enzyme assay. Compound **8** was discovered to function as an H-bond acceptor from amino acid **Lys200** as well as an H-bond donor to **Glu233**. The interaction between compound **8** and **His101** was shown to be H-arene. Compound **6** displayed three H-bonds with the binding pocket, as well as three arene-H interactions with **His305** and **Gly306**. Table 13 provides a summary of ligand interactions. Compound **16** revealed two H-arene contacts with **Trp59**, one H-bond with **Gln63**, and two arene-H interactions with **Leu162**. Compound **4** had just one arene-H interaction with **Gly306**, and it had the greatest energy score of −7.93 kCal/mol. Figure 4 shows ligand interactions and binding modalities.

Moreover, compounds **6** and **8** showed the lowest energy in the case of *α*-glucosidase, with score values of −10.63 and −10.79 kCal/mol, respectively. This demonstrates that it agrees with the findings of the enzyme assay. Compound **6** was discovered to function as an H-bond acceptor from the amino acids **Trp481** and **His674** as well as an H-bond donor to the amino acids **Asp616** and **Asp645**. Compound **8** revealed the same ligand interactions with the same amino acids as compound **6** (shown in Figure 5), in addition to a comparable manner of contact. However, compound **8** demonstrated an additional arene-H interaction with **Leu283**. Table 13 provides a summary of ligand interactions. Compound **16** had a score of −9.37 kCal/mol, which was slightly higher than average in terms of energy. It displayed three contacts with **Asp616**, **Asp645**, and **Trp481** as well as an additional arene-H interaction with **Leu83**, which were shared by compounds **6** and **8** as well. With just one H-bond to **His674**, compound **4** has the highest energy score, measuring −7.83 kCal/mol.

Conclusion

A series of novel indenoquinoxaline, Schiff's base derivatives **4–6**, hydrazone derivatives **7–9**, arylidine-indenoquinoxaline derivatives **10**, **12**, and **13**, and thiazole derivatives **15–17** was designed, synthesised, and subjected to biological evaluation as antidiabetic agents. The results indicated that there are four hybrids with good activity. Compounds **4**, **6**, **8**, and **16** possess promising antidiabetic properties demonstrated by decreasing glucose level, increasing insulin level, also causes inhibition of *α*-amylase and *α*-glucosidase activities. In addition to their antioxidant, hypocholesteremic, renoprotective and hepatoprotective properties. When compared to acarbose, a reference medication (IC_{50}=0.316±0.02 and 31.56±1.33 μM), the four compounds showed moderate to powerful activity with IC_{50} values of 0.982±0.04, 10.19±0.21, 17.58±0.74, and 121.6±5.14 μM, respectively. The Schiff base derivative **6** and the hydrazone derivative **8** demonstrate the importance of these moieties for the anti-diabetic actions as these derivatives show the best result when compared to the standard acarbose as *α*-amylase & *α*-glucosidase inhibitors. In addition, docking experiments were used to confirm the binding interactions, and all hybrid and standard medicines underwent in silico ADME and toxicity tests. Future work will be done for the most promising hybrids **6** and **8**, to study another mode of actions as well as formulation in different dosage form to be tested.

Ethical approval

The least number of animals necessary to attain statistical significance was used. Mice were housed under a 12-hour light/dark cycle; a relative humidity of 50%; and a controlled temperature of 22±1 ℃; with free access to food and water. At the end of

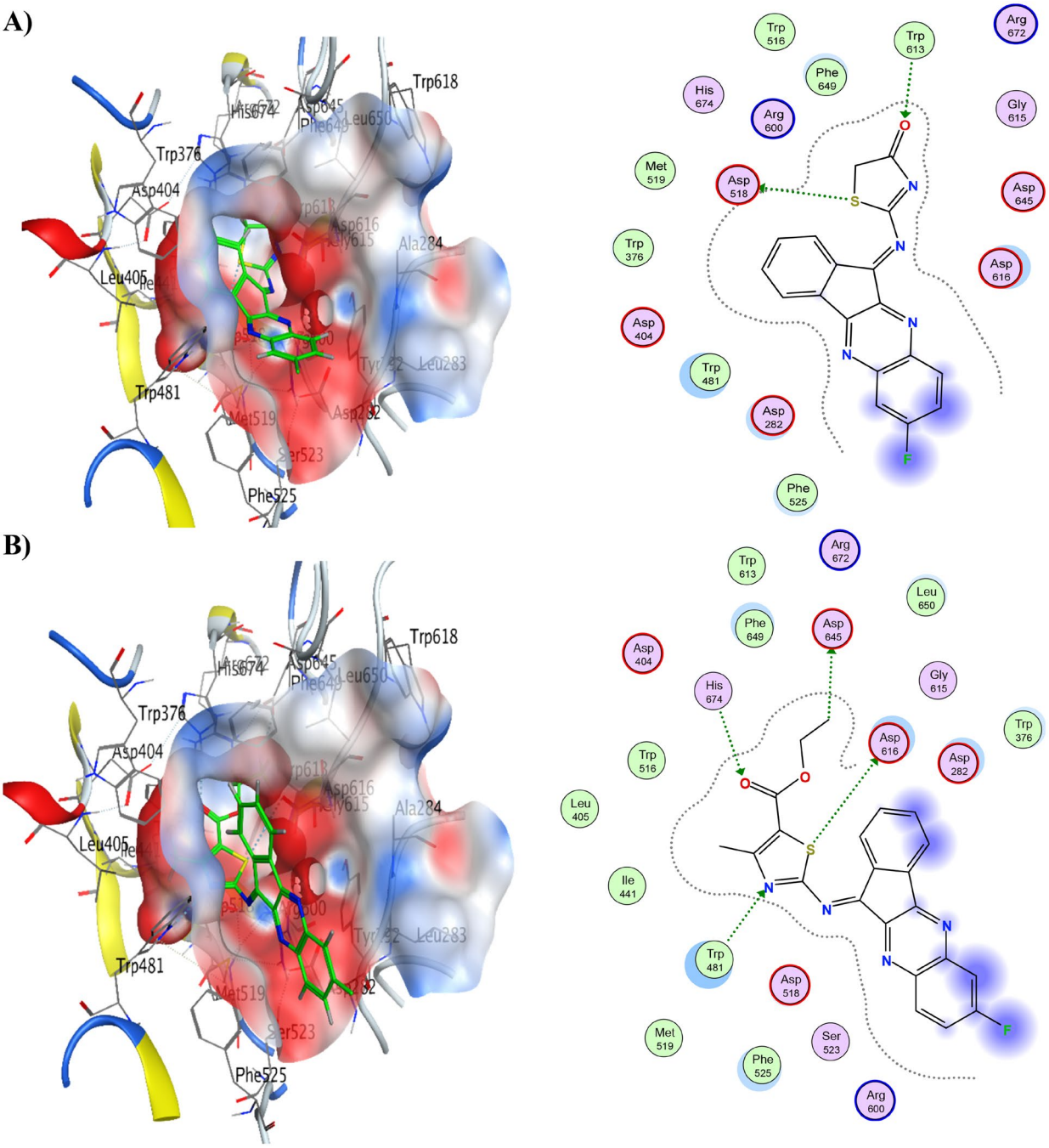

Figure 5. 3D binding modes & 2D ligand interactions with *α*-glucosidase (PDB ID: 5NN8) of the most active compounds, (A) Compound 4, (B) Compound 6, (C) Compound 8, (D) Compound 16.

the experiment, mice were euthanatized by cervical dislocation. The protocol of the current research study is in line with the ARRIVE guidelines for the use and care of laboratory animals and approved by the research ethics committee for experimental and clinical studies at the Faculty of Pharmacy (Girls), Al-Azhar University (Permit number: ES 408, 1/6/2023).

Authors' contributions

Conceptualisation, E.A.F., A.R., Y.A.A., A.M.M., and M.S.A.; Data curation, N.A.G., E.A.F., A.R., O.A.A.A., Y.A.A., A.M. M., and M.S.A.; Formal analysis, N.A.G., E.A.F., A.R., O.A.A.A., A.M. M., and M.S.A.; Investigation, N.A.G., E.A.F., A.R., O.A.A.A., Y.A.A. and M.S.A.; Methodology, N.A.G., E.A.F., A.R., A.M.M., and M.S.A.; Project administration, Y.A.A., and E.A.F.; Resources, E.A.F., O.A.A.A.; Software, E.A.F.; Supervision, E.A.F., Y.A.A.; Validation, E.A.F., and A.M.M.; Writing—original draft, E.A.F., N.A.G., A.R., A.M. M., and M.S.A.; Writing—review & editing, E.A.F., N.A.G., A.R. and M.S.A. All authors have read and agreed to the published version of the manuscript.

Institutional review board statement

Not applicable.

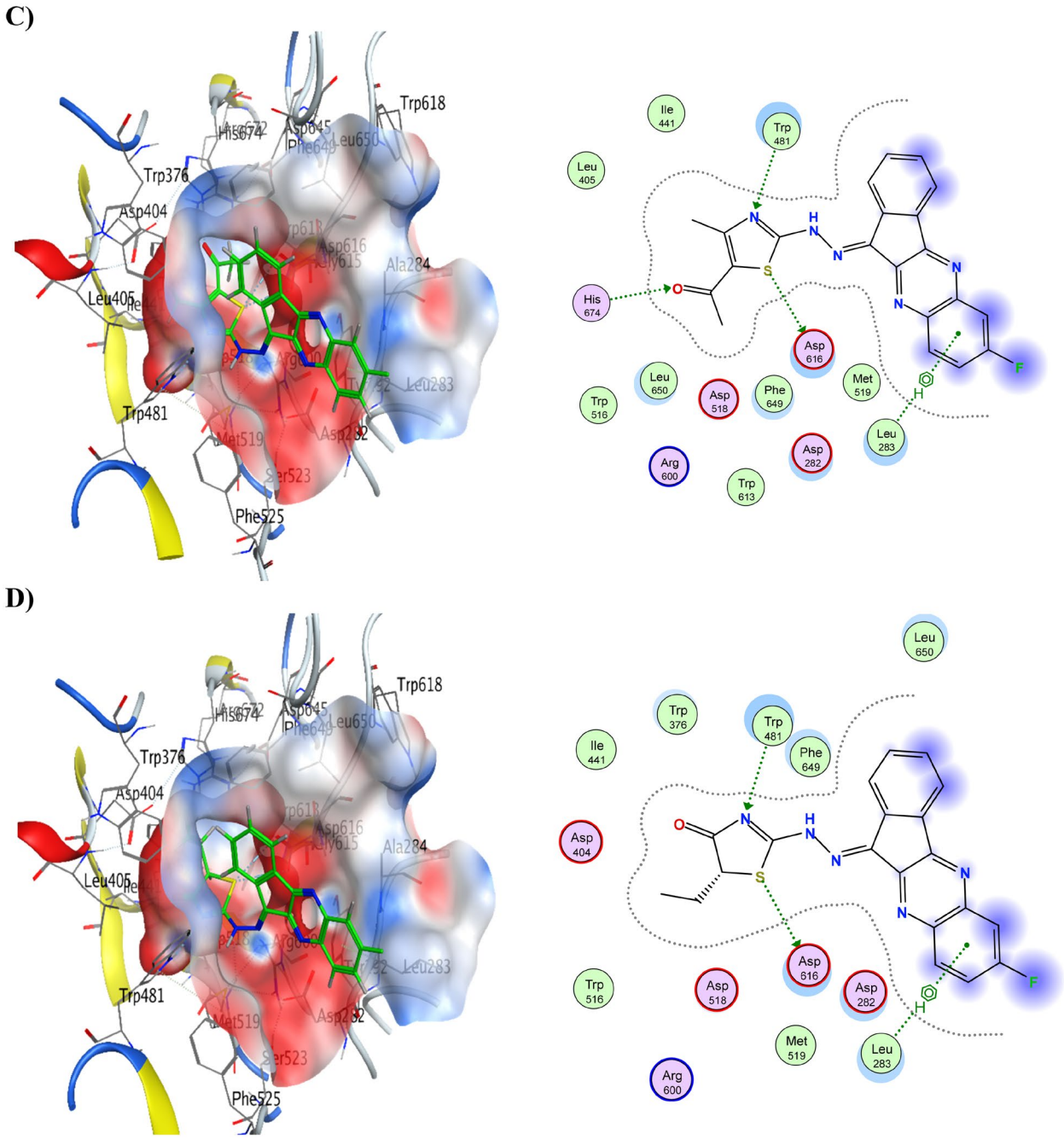

Figure 5. Continued.

Informed consent statement

Not applicable.

Disclosure statement

No potential conflict of interest was reported by the author(s).

Funding

The project has been funded by the Taif University Researchers Supporting Project (TURSP) at Taif University, Taif, Saudi Arabia, under Grant (TURSP-2020/220). The authors extend their appreciation to Tife University, Saudi Arabia, for supporting this work through project number (TU-DSPP-2024-85).

Data availability statement

Data is contained within the article and supplementary material.

References

1. World Health Organization. Definition, diagnosis and classification of diabetes mellitus and its complications: Report of a who consultation. Part 1, diagnosis and classification of diabetes mellitus. In. Definition, diagnosis and classification of

diabetes mellitus and its complications: Report of a who consultation. Part 1, Diagnosis and Classification of Diabetes Mellitus: World Health Organization. 1999;25:1–17.
2. Adaikalakoteswari A, Balasubramanyam M, Mohan V. Telomere shortening occurs in Asian Indian type 2 diabetic patients. Diabetic Med. 2005;22(9):1151–1156.
3. Miles PD, Levisetti M, Reichart D, Khoursheed M, Moossa A, Olefsky JM. Kinetics of insulin action in vivo: identification of rate-limiting steps. Diabetes. 1995;44(8):947–953.
4. Xu J, Zou M-H. Molecular insights and therapeutic targets for diabetic endothelial dysfunction. Circulation. 2009;120(13):1266–1286.
5. Mahfoz AM, Hassanein NM, Shoka AA, El-Latif A, Hekma A. Diabetic nephropathy: Review of novel experimental and clinical strategies. Bull Fac Pharm Cairo Univ. 2019;57(2):127–136.
6. El Maleky W, Mahfoz AM, Osman AO, Abd El-Latif HA. Investigation of the impacts of zamzam water on streptozotocin-induced diabetic nephropathy in rats. in-vivo and in-vitro study. Biomed Pharmacother . 2021;138:111474.
7. Mehmood R, Mughal EU, Elkaeed EB, Obaid RJ, Nazir Y, Al-Ghulikah HA, Naeem N, Al-Rooqi MM, Ahmed SA, Shah SWA, et al. Synthesis of novel 2, 3-dihydro-1, 5-benzothiazepines as α-glucosidase inhibitors: In vitro, in vivo, kinetic, sar, molecular docking, and qsar studies. ACS Omega. 2022;7(34):30215–30232.
8. Jarald E, Joshi SB, Jain DC. Diabetes and Herbal Medicines. IJPT. 2008;7(1):97–106.
9. Henrissat B, Bairoch A. New families in the classification of glycosyl hydrolases based on amino acid sequence similarities. Biochem J. 1993;293 (Pt 3) (Pt 3):781–788.
10. Dauw CA, Simeon L, Alruwaily AF, Sanguedolce F, Hollingsworth JM, Roberts WW, Faerber GJ, Wolf JS, Jr, Ghani KR. Contemporary practice patterns of flexible ureteroscopy for treating renal stones: Results of a worldwide survey. J Endourol. 2015;29(11):1221–1230.
11. Sales PMD, PMd S, Simeoni LA, PdOMD B, Silveira D. A-amylase inhibitors: a review of raw material and isolated compounds from plant source. J Pharm Pharm Sci. 2012;15(1):141–183.
12. Nair SS, Kavrekar V, Mishra A. In vitro studies on alpha amylase and alpha glucosidase inhibitory activities of selected plant extracts. Eur J Exp Biol. 2013;3(1):128–132.
13. Sundarram A, Murthy TPK. A-amylase production and applications: a review. J Appl Environ Microbiol. 2014;2(4):166–175.
14. Taha M, Javid MT, Imran S, Selvaraj M, Chigurupati S, Ullah H, Rahim F, Khan F, Mohammad JI, Khan KM. Synthesis and study of the α-amylase inhibitory potential of thiadiazole quinoline derivatives. Bioorg Chem. 2017;74(:179–186.
15. Petrou A, Fesatidou M, Geronikaki A. Thiazole ring—a biologically active scaffold. Molecules. 2021; 26(11):3166.
16. Xie Z, Wang G, Wang J, Chen M, Peng Y, Li L, Deng B, Chen S, Li W. Synthesis, biological evaluation, and molecular docking studies of novel isatin-thiazole derivatives as α-glucosidase inhibitors. Molecules. 2017;22(4):659.
17. Wang G, He D, Li X, Li J, Peng Z. Design, synthesis and biological evaluation of novel coumarin thiazole derivatives as α-glucosidase inhibitors. Bioorg Chem. 2016;65(:167–174.
18. Ghani U, Albarrag A, Yurttaş L, Demirci F, Kaplancikli ZA. Carbazoles and hydrazone-bridged thiazole-pyrrole derivatives as new inhibitors of α-glucosidase. ChemistrySelect. 2018;3(27):7921–7925.
19. Wang G, Peng Z, Gong Z, Li Y. Synthesis, biological evaluation, and docking studies of novel 5, 6-diaryl-1, 2, 4-triazine thiazole derivatives as a new class of α-glucosidase inhibitors. Bioorg Chem. 2018;78:195–200.
20. Kumar H, Dhameja M, Kurella S, Uma A, Gupta P. Synthesis, in-vitro α-glucosidase inhibition and molecular docking studies of 1, 3, 4-thiadiazole-5, 6-diphenyl-1, 2, 4-triazine hybrids: Potential leads in the search of new antidiabetic drugs. J Mol Struct . 2023;1273(:134339.
21. Mahapatra T, Nanda S. Asymmetric synthesis of hydroxy-skipped bishomo-inositols as potential glycosidase inhibitors. Tetrahedron: Asymmetry. 2010;21(18):2199–2205.
22. AbdelFattah BA, Khalifa MMA, El-Sehrawi H, Fayed E, Bayoumi A, Said M. Synthesis and anxiolytic activity of some novel 5-oxo-1, 4-oxazepine derivatives. LDDD. 2011;8(4):330–338.
23. Fayed EA, Ahmed HY. Synthesis, characterization and pharmacological evaluation of some new 1, 4-diazepine derivatives as anticancer agents. Der Pharma Chem. 2016;8(13):77–90.
24. Fathy U, Abd El Salam HA, Fayed EA, Elgamal AM, Gouda A. Facile synthesis and in vitro anticancer evaluation of a new series of tetrahydroquinoline. Heliyon. 2021;7(10): e08117.
25. Othman EM, Fayed EA, Husseiny EM, Abulkhair HS. Rationale design, synthesis, cytotoxicity evaluation, and in silico mechanistic studies of novel 1, 2, 3-triazoles with potential anticancer activity. New J Chem. 2022;46(25):12206–12216.
26. Ammar YA, Fayed EA, Bayoumi AH, Ezz RR, Alsaid MS, Soliman AM, Ghorab MM. New chalcones bearing isatin scaffold: synthesis, molecular modeling and biological evaluation as anticancer agents. Res Chem Intermed. 2017; 43(12) :6765–6786.
27. Ramsis TM, Ebrahim MA, Fayed EA. Synthetic coumarin derivatives with anticoagulation and antiplatelet aggregation inhibitory effects. Med Chem Res. 2023;32(11):2269–2278.
28. Trinder P. Determination of blood glucose using an oxidase-peroxidase system with a non-carcinogenic chromogen. J Clin Pathol. 1969; 22(2):158–161.
29. Orsonneau J-L, Massoubre C, Cabanes M, Lustenberger P. Simple and sensitive determination of urea in serum and urine. Clin Chem. 1992;38(5):619–623.
30. Saibaba K, Srinivasa Rao P, Dakshina Murty K, Bhaskar MV. Method evaluation of an enzymatic method for serum creatinine. Indian J Clin Biochem. 1997;12(2):139–141.
31. Beutler E, Duron O, Kelly BM. Improved method for the determination of blood glutathione. J Lab Clin Med. 1963; 61(:882–888.
32. Kei S. Serum lipid peroxide in cerebrovascular disorders determined by a new colorimetric method. Clin Chim Acta. 1978;90(1):37–43.
33. Piyachaturawat P, Poprasit J, Glinsukon T, Wanichanon C. Gastric mucosal lesions in streptozotocin-diabetic rats. Cell Biol Int Rep. 1988;12(1):53–63.
34. Walker HK, Hall WD, Hurst JW. Clinical methods: the history, physical, and laboratory examinations. 3rd ed. Boston: Butterworths; 1990.
35. McCue PP, Shetty K. Inhibitory effects of rosmarinic acid extracts on porcine pancreatic amylase in vitro. Asia Pac J Clin Nutr. 2004;13(1):101–106.
36. Daina A, Michielin O, Zoete V. Swissadme: a free web tool to evaluate pharmacokinetics, drug-likeness and medicinal chemistry friendliness of small molecules. Sci Rep. 2017;7(1):42717.

37. Kar S, Roy K, Leszczynski J. In silico tools and software to predict admet of new drug candidates. In: In silico methods for predicting drug toxicity. New York (NY): Springer US; 2022. p. 85–115.
38. Refai MY, Elazzazy AM, Desouky SE, Abu-Elghait M, Fayed EA, Alajel SM, Alajlan AA, Albureikan MO, Nakayama J. Interception of epoxide ring to quorum sensing system in enterococcus faecalis and staphylococcus aureus. AMB Express. 2023;13(1):126.
39. Fayed EA, Thabet A, Abd El-Gilil SM, Elsanhory HM, Ammar YA. Fluorinated thiazole–thiosemicarbazones hybrids as potential ppar-γ agonist and α-amylase, α-glucosidase antagonists: design, synthesis, in silico admet and docking studies and hypoglycemic evaluation. J Mol Struct . 2024;1301:137374.
40. Fayed EA, Al-Arab EME, Saleh AS, Bayoumi AH, Ammar YA. Design, synthesis, in silico studies, in vivo and in vitro assessment of pyridones and thiazolidinones as anti-inflammatory, antipyretic and ulcerogenic hits. J Mol Struct. 2022;1260: 132839.
41. Fayed EA, Gohar NA, Farrag AM, Ammar YA. Upregulation of bax and caspase-3, as well as downregulation of bcl-2 during treatment with indeno [1, 2-b] quinoxalin derivatives, mediated apoptosis in human cancer cells. Arch Pharm. 2022;355 (5):e2100454.
42. Bax BD, Chan PF, Eggleston DS, Fosberry A, Gentry DR, Gorrec F, Giordano I, Hann MM, Hennessy A, Hibbs M, et al. Type iia topoisomerase inhibition by a new class of antibacterial agents. Nature. 2010;466(7309):935–940.
43. Fayed EA, Nosseir ES, Atef A, El Kalyoubi SA. In vitro antimicrobial evaluation and in silico studies of coumarin derivatives tagged with pyrano-pyridine and pyrano-pyrimidine moieties as DNA gyrase inhibitors. Mol Divers. 2022;26(1):341–363.
44. Fayed EA, Ebrahim MA, Fathy U, El Saeed HS, Khalaf WS. Evaluation of quinoxaline derivatives as potential ergosterol biosynthesis inhibitors: design, synthesis, admet, molecular docking studies, and antifungal activities. J Mol Struct . 2022;1267:133578.
45. Othman EM, Fayed EA, Husseiny EM, Abulkhair HS. The effect of novel synthetic semicarbazone-and thiosemicarbazone-linked 1, 2, 3-triazoles on the apoptotic markers, vegfr-2, and cell cycle of myeloid leukemia. Bioorg Chem. 2022;127:105968.
46. Desouky SE, Abu-Elghait M, Fayed EA, Selim S, Yousuf B, Igarashi Y, Abdel-Wahab BA, Mohammed Alsuhaibani A, Sonomoto K, Nakayama J. Secondary metabolites of actinomycetales as potent quorum sensing inhibitors targeting gram-positive pathogens: in vitro and in silico study. Metabolites. 2022;12(3):246.
47. Fayed EA, Gohar NA, Bayoumi AH, Ammar YA. Novel fluorinated pyrazole-based heterocycles scaffold: cytotoxicity, in silico studies and molecular modelling targeting double mutant egfr l858r/t790m as antiproliferative and apoptotic agents. Med Chem Res. 2023;32(2):369–388.
48. Fayed EA, Ebrahim MA, Fathy U, Elawady AM, Khalaf WS, Ramsis TM. Pyrano-coumarin hybrids as potential antimicrobial agents against mrsa strains: design, synthesis, admet, molecular docking studies, as DNA gyrase inhibitors. J Mol Struct . 2024;1295:136663.
49. Ahangarpour A, Heidari H, Oroojan AA, Mirzavandi F, Esfehani KN, Mohammadi ZD. Antidiabetic, hypolipidemic and hepatoprotective effects of arctium lappa root's hydro-alcoholic extract on nicotinamide-streptozotocin induced type 2 model of diabetes in male mice. Avicenna J Phytomed. 2017;7(2):169.
50. Ragab A, Abusaif MS, Gohar NA, Aboul-Magd DS, Fayed EA, Ammar YA. Development of new spiro [1, 3] dithiine-4, 11′-indeno [1, 2-b] quinoxaline derivatives as s. Aureus sortase a inhibitors and radiosterilization with molecular modeling simulation. Bioorg Chem. 2023;131:106307.
51. Raghuvanshi DS, Singh KN. Microwave-assisted synthesis of some novel thiazolidinone and thiohydantoin derivatives of isatins. Phosphorus, Sulfur, Silicon Relat Elem. 2010;185(11): 2243–2248.
52. K Ramshid P, Jagadeeshan S, Krishnan A, Mathew M, Asha Nair S, Radhakrishna Pillai M. Synthesis and in vitro evaluation of some isatin-thiazolidinone hybrid analogues as anti-proliferative agents. MC. 2010;6(5):306–312.